

# Surface charge on sago starch granules

Shun Nishiyama<sup>1\*</sup>, Masanori Okazaki<sup>1</sup>, Naoya Katsumi<sup>1</sup>,  
Yuji Honda<sup>1</sup> and Mayuko Tsujimoto<sup>2</sup>

<sup>1</sup>Ishikawa Prefectural University, 1-308, Suematsu, Nonouchi, Ishikawa 921-8836 Japan

<sup>2</sup>Tokyo University of Agriculture and Technology, 2-24-16, Nakacho, Koganei, Tokyo 184-8588 Japan

\*Corresponding author

**Abstract:** Knowing the characteristics of sago starch is necessary for the development of sago utilization. The mean diameter and nanostructure are characteristics of sago starch important for flocculation and dispersion, useful in printing, manufacturing paper and corrugated cardboard, and other industries. Sago starch granules are oval and bell shaped, with 37.59  $\mu\text{m}$  of mean diameter in water and 37.73 to 38.27  $\mu\text{m}$  in 0.01, 0.1, and 1  $\text{mol L}^{-1}$   $\text{NaClO}_4$  solution, which showed a C-type (mainly A-type (monoclinic) with B-type (hexagonal) as an accessory) X-ray diffraction pattern. Sago starch showed variable charge, and the surface charge of sago starch granules ranged from positive to negative with a point of zero charge at pH 6.1 in 0.1  $\text{mol L}^{-1}$   $\text{NaClO}_4$  solution. These results indicate that sago starch had the intermediate dynamics of a point of zero charge as compared to corn (pH 4.7) and potato starches (pH 6.0).

**Keywords:** infrared absorption, NMR, sago starch, surface charge

## Introduction

The sago palm (*Metroxylon sagu* Rottb.), grown in the lowlands of Southeast Asia, is a useful plant that can accumulate up to 200 kg of starch per palm. Foods, paper, cardboard, ink, and other goods are produced from sago starch (Hidaka et al., 2010; Fukino, 2000). Japan annually imports 20 thousands ton of sago starch as dusting flour, mainly from Malaysia and Indonesia (Agriculture and Livestock Industries Corporation, 2014). Sago starch is oval or bell shaped with a mean diameter of 31.0  $\mu\text{m}$  (Kobayashi, 1993) and a granular size distribution of two peaks, 15 and 30  $\mu\text{m}$  in diameter (Hamanishi et al., 2005). The amylose content in sago starch was 26 %, which is similar to that of corn starch (Takahashi et al., 1995). The distribution profile of unit-chain length of debranched sago amylopectin analyzed by fluorophore-assisted capillary electrophoresis showed a maximum at degree of polymerization (PD) 11-12 (Srichuwong et al., 2005). Phosphate is an important starch component of phosphoric esters, such as amylopectin and phospholipids, in starch granules. In addition, phosphoric ester gives positive and negative

charges to amylopectin and controls the surface charge on starch granules and the behavior of water molecules in the structure of starch. Wongsagonsup et al. (2005) showed zeta potential on the surface of rice starch and suggested that the phosphate in rice starch provided a negative charge and colloidal stability.

When paper was primarily made of fibers, starches were traditionally used to impart dry strength and enhance the surface integrity for improved writing and printing. Paper and cardboard also have negative charges due to the cellulose OH group. The negative surface charges on starch and paper caused the repulsion of both. Accordingly, the cationic functional groups, tertiary amines and/or quaternary ammonium cations, were introduced to starch to make the positive surface charge (Wang et al., 2009).

The objective of this study is to elucidate the surface charge on sago starch and its implication for multiple utilizations.

## Materials and Methods

### 1. Sago starch

Sago starch samples were collected in Hilsig, Leyte,

Philippines, in 2009 (Okazaki et al., 2013). Sago starch grains were extracted from the pith pulp by washing with water after grating. Corn (Kosakai Pharmaceutical Co.) and potato starches (Miyazawa Pharmaceutical Co.) certified by The Japanese Pharmacopoeia were used as references.

## 2. Observation of starch appearance

Sago starch samples dispersed in water and air-dried sago starch samples were observed by an optical microscope (MT 9300, Meiji Techno) and a scanning electron microscope (Miniscope TM-1000, Hitachi), respectively.

## 3. X-ray diffraction pattern and crystalline properties of sago starch

The X-ray diffraction pattern of sago starch samples was obtained by an X-ray diffractometer (MiniFlex, Rigaku). The measurement conditions are as follows: Cu tube, Ni filter, 30 kV, 15 mA, operation angle  $0$  to  $45$  degree for  $2\theta$ . The crystalline index of sago starch was calculated by the following equation:

$$\text{Crystalline index} = (\text{peak height}_{3b} / \text{FWHM}_{3b} + \text{peak height}_{4a} / \text{FWHM}_{4a}) \cdot (1)$$

FWHM: full width at half maximum

which was referred to by Katsumi et al. (2014).

## 4. Particle-size distribution of sago starch

The particle-size distributions of sago starch samples after sonication for 10 seconds at 150 W were determined using the Coulter Principle, also known as the Electrical Sensing Zone (Multisizer 4, Beckman Coulter) in water, which provided the starch particle-size distribution in number and volume, and using laser diffraction and light scattering methods (LS 13 320, Beckman Coulter) in 0.01, 0.1, and 1 mol L<sup>-1</sup> NaClO<sub>4</sub>. Particle-size distribution was determined using 100 mg in 125 mL for Multisizer 4 and 100 mg in 100 mL for LS 13 320.

## 5. Infrared absorption of sago starch

Functional group analysis of sago starch was carried out using KBr plates with a Fourier Transform Infrared Spectroscopy Microscope (Jasco IRT-3000), aperture size 5 x 5 x 1 mm, total number measured 128, with background correction. The sago starch granule was observed by a CCD monitor type after setting the sample position and aperture size.

## 6. Solid-state <sup>13</sup>C-NMR of sago starch

A Jeol Detum ECA/ECX solid-state CP/MAS <sup>13</sup>C NMR spectrometer was operated at a <sup>13</sup>C-resonance frequency of 500 MHz, a spinning rate of 10 kHz, and a point number of 2048, using scanning numbers 128 and 256, at room temperature.

## 7. Chemical properties of sago starch

The pH and phosphate concentrations of sago starch samples were determined using a pH meter (pH meter M-13, Horiba) and using a spectrophotometer (UVmini 1240, Shimadzu) by a molybdenum blue procedure (Hokkaido Branch of The Chemical Society of Japan, 1996), respectively. The pH values and phosphate concentration affect the surface charge and the behavior of sago starch in solution.

## 8. Surface charge of sago starch

The surface charge of sago starch was determined by the titration method of Schultheiss and Sparks (1986). Starch granules were suspended in 0.01 mol L<sup>-1</sup> NaClO<sub>4</sub> solution and titrated with HClO<sub>4</sub> and NaOH using an automatic titrator (Auto Titrator COM-1600, K-2000 Stirrer and Buret B-2000, Hiranuma).

## Results and Discussion

### 1. Observation of starch appearance

Sago starch granules are oval or polygonally shaped with a number of truncated granules (Takahashi et al., 1995; Karim et al., 2008). Figure 1 shows sago starch granules under a microscope from our experiments. Sago starch samples were oval and bell shaped, which corresponded to the results of

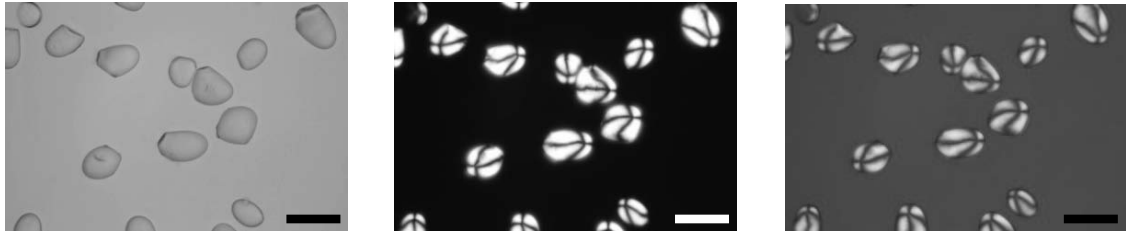


**Fig. 1.** Sago starch grains under polarized microscope  
Bar shows 50 µm.

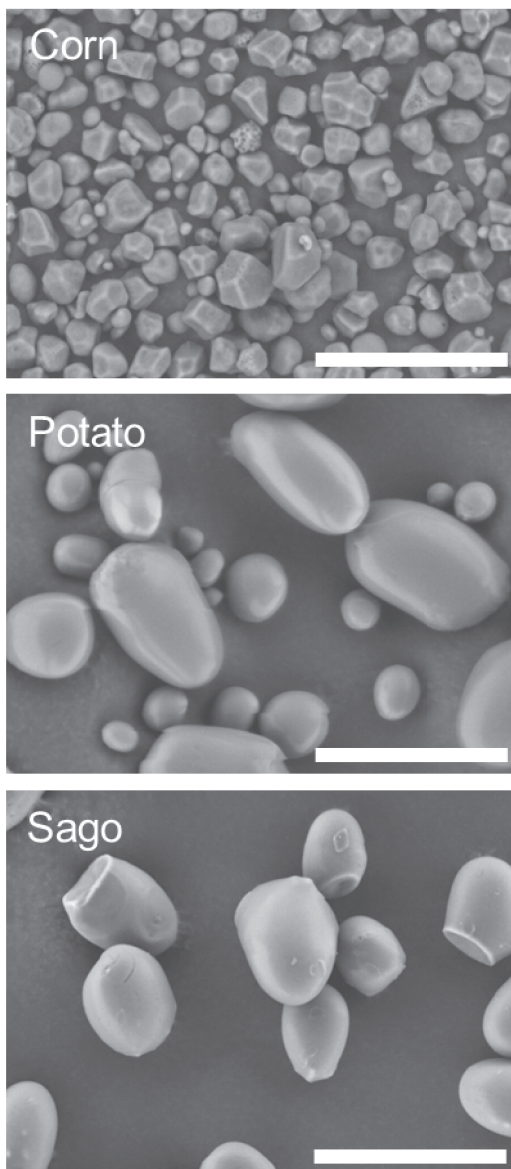


**Fig. 2.** Electron microscope image of corn, potato, and sago starches  
Bar shows 50 µm.

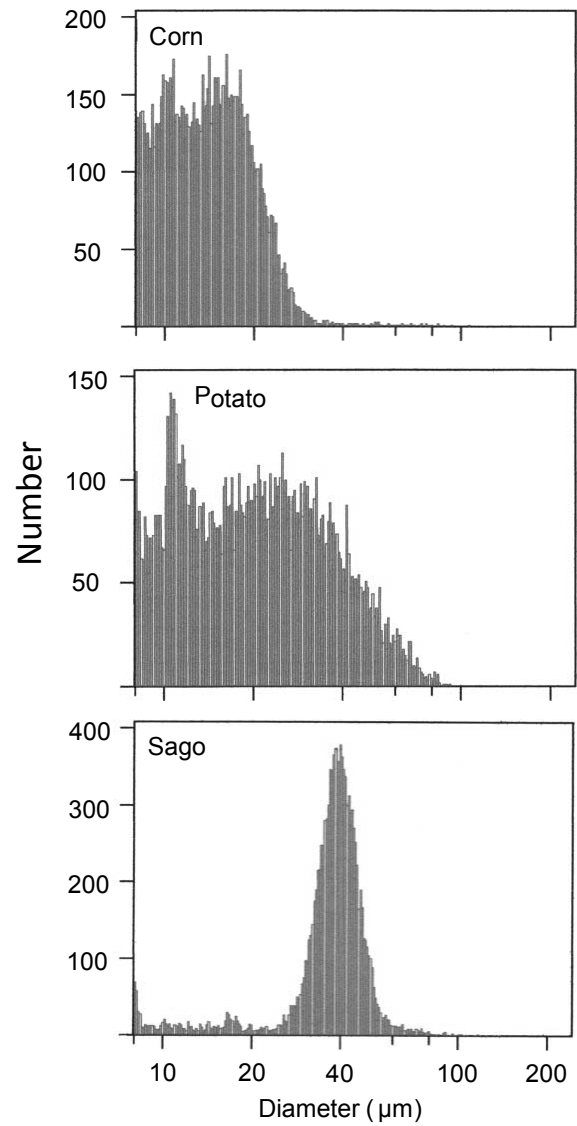


**Fig. 3.** Particle-size distribution of corn, potato, and sago starches

Karim et al. (2008). Kawagoe (2013) suggested that the stroma developed the septum-like structure in an amyloplast and finally produced bell shapes. The sago starch granules exhibited a Maltese cross under crossed nicols, indicating the presence of the crystalline structure of amylose and amylopectin. Figure 2 shows the appearance of corn, potato, and sago starch granules under a scanning electron microscope. Sago starch clearly has a bell shape.

## 2. Particle-size distribution of sago starch

The mean particle size of sago (8 to 240  $\mu\text{m}$ ) was 37.59  $\mu\text{m}$  with a standard deviation of  $\pm 11.0 \mu\text{m}$  and 29.3 % for the coefficient of variation (Fig. 3), which was relatively larger than the result of Kobayashi (1993). The distribution of the sago starch grain size showed the normal distribution with the tailing of small granules. Corn and potato starches were characterized by the bimodal size distribution with mean particle sizes of 14.76  $\mu\text{m}$  and 23.70  $\mu\text{m}$ , respectively, which were smaller mean particle sizes than that of sago starch. Lim et al. (1992) showed that the mean particle sizes of corn and potato starches were 14.3  $\mu\text{m}$  and 35.0  $\mu\text{m}$ , respectively. The potato starch (permitted under Japanese pharmacopoeia) used in our experiment was smaller than that used by Lim et al. (1992).

## 3. X-ray diffraction pattern and crystalline properties of sago starch

The X-ray diffraction pattern of sago starch (Fig. 4) indicates peaks at around 5.6, 17, 18, and 23 degrees, corresponding to 1.6, 0.52, 0.49, and 0.39 nm, respectively, which are classified as CA starches (Cai et al., 2014), a mixture of A- and B-types of starches. This is similar to the results of Okazaki et al. (2008). Sago starch is classified

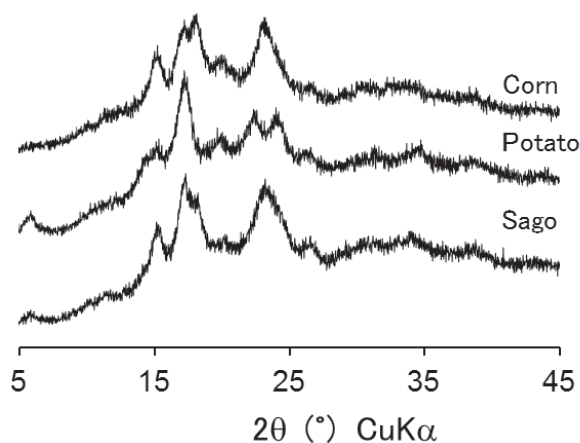


**Fig. 4.** X-ray diffraction pattern of corn, potato, and sago starches

as a C type, containing mainly A-type and B-type as an accessory. Corn and potato starches gave typical A- and B-type X-ray diffraction patterns. The crystalline index of sago starch was 610 (Table 1), calculated by equation (1) (Katsumi et al., 2014). These samples were the same as those of Katsumi et al. (2014) and were different specimens from the same samples.

## 4. Infrared absorption

Infrared absorption spectra of sago starches shown in Fig. 5 exhibit the O-H stretching vibration of water molecules and the O-H of starch at 3600–3200  $\text{cm}^{-1}$ , aliphatic C-H stretching vibration at 3100–2800  $\text{cm}^{-1}$ , OH bending vibration at 1600  $\text{cm}^{-1}$ , and aliphatic C-H bending vibration at 1500–1300  $\text{cm}^{-1}$ ; absorption at 1200–1000  $\text{cm}^{-1}$  was attributed to the C-O bond-stretching vibration of the anhydroglucose units (Wang et al., 2009). Corn and potato starches showed infrared absorption spectra similar to that of sago starch.

**Table 1.** Chemical properties of sago starch

	pH (H <sub>2</sub> O,1:5)	Phosphate concentration mg kg <sup>-1</sup>		Crystalline index
		This study	Misaki and Kakuta (2003)	
Corn	4.44	140	150	920
Potato	7.65	500	830	880
Sago	5.87	80	-	610

Crystalline index: peak height<sub>3b</sub> / FWHM<sub>3b</sub> + peak height<sub>4a</sub> / FWHM<sub>4a</sub> (Katsumi et al., 2014)

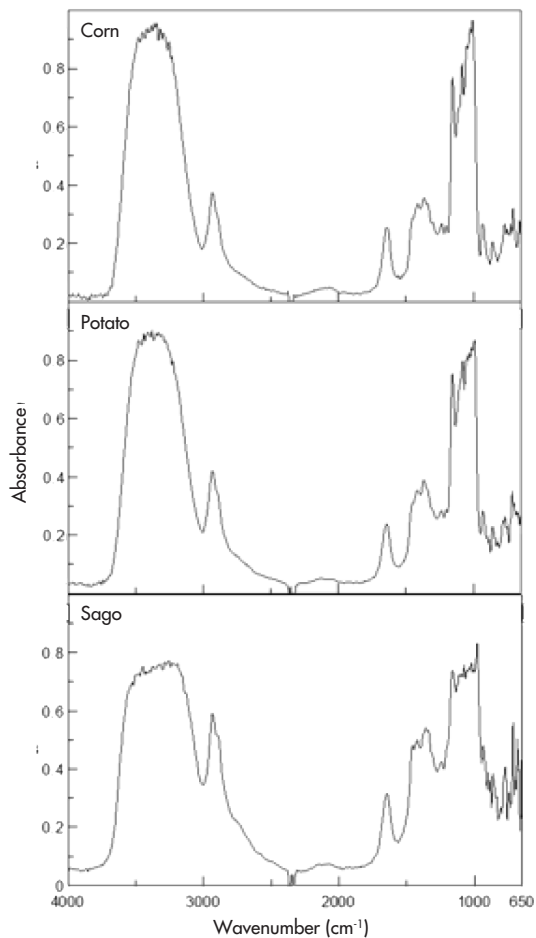


Fig. 5. Infrared spectrum of corn, potato, and sago starches

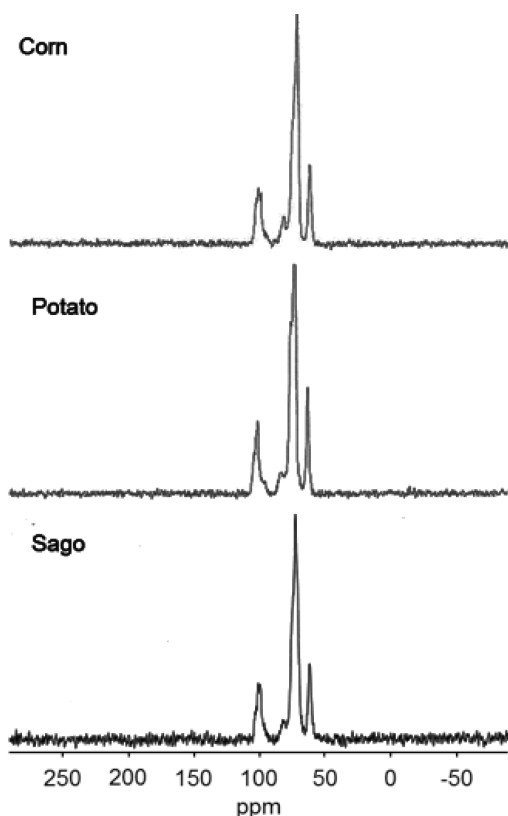


Fig. 6.  $^{13}\text{C}$ -NMR spectra of corn, potato, and sago starches

## 5. Solid-state $^{13}\text{C}$ -NMR

Solid-state  $^{13}\text{C}$ -NMR spectra of sago starch granules show the resonance at around 102, 85, 80 to 78, and 70 ppm (Fig. 6). The C1 site of individual glucose units in sago starch provided the resonance at 103, 102 and 100 ppm. The C4 site gave 85 ppm. Eighty to 78 ppm was assigned to the C2, C3, and C5 sites. The C6 site gave 70 ppm (Gidley and Bociek, 1985). The A-type starch (corn starch) structure exhibited three peaks at 103, 102 and 100 ppm. There was no significant difference in solid-state  $^{13}\text{C}$ -NMR spectra between corn and sago starches.

## 6. Surface charge of sago starch

The surface charge of sago starch shown in the 0.1 mol L<sup>-1</sup> NaClO<sub>4</sub> (Fig. 7) was derived from phosphoric ester; 60 to 70 % of total phosphate was present at C6 and 30 % at C3 of the glucose residue (Misaki and

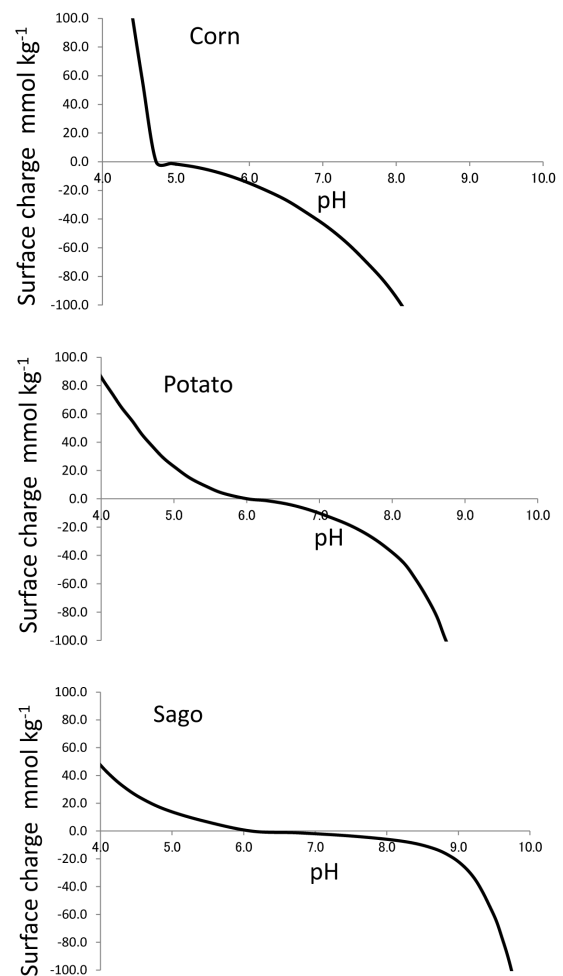


Fig. 7. Surface charges of corn, potato, and sago starch granules



Kakuta, 2003). Phosphoric ester in the starch gave the positive charge, ranging from 0 to 50 mmol/kg<sup>-1</sup> for sago starch, in the pH range below pH 6.1, and the negative charge was also provided in the range of pH 6.1 to 9 from 0 to -20 mmol kg<sup>-1</sup>. These indicate “variable charges” on sago starch. It suggested that phosphoric esters in sago starch in the 0.1 mol L<sup>-1</sup> NaClO<sub>4</sub> solution might be dissociated according to their dissociation constant and emerged at the adsorption sites for H<sup>+</sup> and OH<sup>-</sup> ions as charge-determining ions (Schultheiss and Sparks, 1986).

The surface charge behavior of sago starch was relatively similar to that of potato starch, while corn starch clearly provided a different surface charge behavior (Fig. 7). Phosphate concentrations, crystalline index (Table 1), and particle-size distribution (Fig. 3) in corn, potato, and sago starches were not directly related to their surface charges. Hatta et al. (2003) showed that the uppermost surface of a sago starch granule (Hatta et al., 2002) resembles the convexo-concave surface of a potato starch, not corn starch. It seems that the surface charge behavior in sago, corn, and potato starches are related to their surface structures.

The electrolyte concentration affected the structure of corn starch granules by means of releasing hydrated water molecules. The surface charge of the sago starch increased as the electrolyte concentration increased in a range of less than 10 wt % (Oostern, 1982; Hirashima, 2007). The structure change may cause the surface charge of starch granules as a result of conformation.

The surface charge of sago starch granules regulates the reaction between granules and between granules and materials, for example, the adsorption of sago starch granules to carboxyl groups on paper and corrugated cardboard. The processing speed of paper and corrugated cardboard machines is controlled by the surface charge of sago starch granule as a surface treatment agent (Jonhed, 2006).

## Conclusion

Sago starch has variable charges that can form strong complexes with positive charge sites on the

materials in the range of above pH 6. Sago starch granules themselves show positive charges below pH 6. Multiple utilizations will be proposed, based on the electrochemical properties of sago starch.

## Acknowledgments

The authors are grateful to Beckman Coulter Ltd. for their support of the analysis of particle-size distribution of sago starch and to Dr. Masato Igura, National Institute of Agro-Environmental Sciences, for his assistance regarding solid-state <sup>13</sup>C NMR.

## References

- Agriculture and Livestock Industries Corporation 2014 Domestic demand of starch in Japan. *Sugar & Starch Information* 24: 35.
- Cai, C. H., J. W. Cai, J. M. Man, Y. Yang, Z. F. Wang and C. X. Wei 2014 Allomorph distribution and granule structure of lotus rhizome C-type starch during gelatinization. *Food Chemistry* 142: 408-415.
- Fukino, H. 2000 Starch and corrugated cardboard manufacturing –Its history and bonding with starch adhesive-. *Journal of Applied Glycoscience* 47: 73-85 (in Japanese).
- Gidley, M. J. and S. M. Bociek 1985 Molecular organization in starches: A <sup>13</sup>C CP/MAS NMR study. *Journal of the American Chemical Society* 107: 7040-7044.
- Hamanishi, T., T. Hatta, F. S. Jong, S. Takahashi and K. Kainuma 2000 Relative crystallization degree, structure and gelatinization of sago starch at different growth stages. *Journal of Applied Glycoscience* 47: 335-341.
- Hamanishi, T., K. Hirao and S. Takahashi 2005 Physicochemical properties of sago starch. *SAGO PALM* 13: 48-51 (in Japanese).
- Hatta, T., S. Nemoto, K. Kainuma, T. Hamanishi, K. Yamamoto, S. Takahashi, K. Kainuma 2002 The uppermost surface structure of sago starch granules. *In: New Frontiers of Sago Palm Studies* (Kainuma, K., M. Okazaki, Y. Toyoda and J. E.

- Cecil eds.) Universal Academy Press (Tokyo) 349-354.
- Hatta, T., S. Nemoto and K. Kainuma 2003 A surface analytical approach to the structure of starch granules. *Japanese Society of Applied Glycoscience* 50:159-162.
- Hidaka, K., T. Sugi and H. Suzuki 2010 Improvement of productivity and quality by preventing starch degradation at papermaking process. *Japan TAPPI Journal* 9: 1-5 (in Japanese).
- Hirashima, M. 2007 Effect of taste substances on cooking characteristics of corn starch. *Journal of Cooney Science of Japan* 40: 47-51 (in Japanese).
- Hokkaido Branch of The Chemical Society of Japan 1996 Phosphate and total phosphorus. *In: Water Analysis. (Kagakudojin, Kyoto)* 323-327, (in Japanese).
- Jonhed, A. 2006 Properties of modified starches and their use in the surface treatment of paper. *Karlstad University Studies* 2006:42: 1-89 at the following URL:  
<http://kau.diva-portal.org/smash/get/diva2:6450/FULLTEXT01.pdf>
- Karim, A. A., A. P-L. Tie, D. M. A. Manan and I. S. M. Zaidul 2008 Starch from the sago (*Metroxylon sago*) palm tree – Properties, prospects, and challenges as a new industrial source for food and other uses. *Comprehensive Reviews in Food Science and Food Safety* 7: 215-228.
- Katsumi, N., M. Okazaki, K. Yonebayashi, F. Kawashima, S. Nishiyama and T. Nishi 2014 New proposal for “crystalline index” of starch. *Sago Palm* 22: 25-30.
- Kawagoe, Y. 2013 Finding the mechanisms of compound type starch formation in rice grain. *Journal of Japan Society for Bioscience, Biotechnology and Agrochemistry* 51: 478-482.
- Kobayashi, S. 1993 Utilizing characteristics of sago palm, *SAGO PALM* 1: 25-32 (in Japanese).
- Lim, S.T., J.L. Jane, S. Rajagopalan and P.A. Seib. 1992 Effect of starch granule size on physical properties of starch-filled polyethylene. *Biotechnology Progress* 8: 51-57
- Misaki, A. and M. Kakuta 2003 Ester reaction. *In: Encyclopedia of Starch Science (Fuwa, E., T. Komaki, S. Hizukiri and K. Kainuma eds.) Asakurashoten (Tokyo)* 142-151.
- Okazaki, M., M. Igura, S. D. Kimura, S. B. Lina, S. Matsumura, T. Nakato, K. Takahashi, M. A. Quevedo and A. B. Loreto 2008 Development of the structure of sago starch. *In: Sago; Its Potential in Food and Industry (Toyoda, Y., M. Okazaki, M. Quevedo and J. Bacusmo eds.) TUAT Press (Tokyo)* 137-143.
- Okazaki, M., K. Yonebayashi, N. Katsumi, F. Kawashima and T. Nishi 2013 Does sago palm have high  $\delta^{13}\text{C}$ ? *Sago Palm* 21: 1-7.
- Oosten, B. J. 1982 Tentative hypothesis to explain how electrolytes affect the gelatinization temperature of starches in water. *Starch* 34: 233-2329.
- Schultheiss, C. P. and D. L. Sparks 1986 Back titration technique for proton isotherm modeling of oxide surfaces. *Soil Science Society of America Journal* 50: 1406-1411.
- Srichuwong, S., T. C. Sunarti, T. Mishima, N. Isono and M. Hisamatsu 2005 Starches from different botanical sources I: Contribution of amylopectin fine structure to thermal properties and enzyme digestibility. *Carbohydrate Polymers* 60: 529-538.
- Takahashi, S., K. Hirao and K. Kainuma 1995 Physico-chemical properties and cooking quality of sago starch. *Sago Palm* 3: 72-82.
- Wang, P. X., X. L. Wu, X. D. Hua, X. Kun, T. Ying, X. B. Du and W. B. Li 2009 Preparation and characterization of cationic corn starch with a high degree of substitution in dioxane-THF-water media. *Carbohydrate Research* 344: 851-855.
- Wongsagonsup, R., S. Shobsngob, B. Oonkhanond and S. Varavinit 2005 Zeta potential ( $\zeta$ ) and pasting properties of phosphorylated or crosslinked rice starches. *Starch/Stärke* 57: 32-37.